

## GRAVITATIONAL INSTABILITIES IN THE DISKS OF MASSIVE PROTOSTARS AS AN EXPLANATION FOR LINEAR DISTRIBUTIONS OF METHANOL MASERS

RICHARD H. DURISEN,<sup>1,2</sup> ANNIE C. MEJIA,<sup>1</sup> BRIAN K. PICKETT,<sup>3</sup> AND THOMAS W. HARTQUIST<sup>4</sup>

*Received 2001 September 21; accepted 2001 November 16; published 2001 December 12*

### ABSTRACT

Evidence suggests that some masers associated with massive protostars may originate in the outer regions of large disks, at radii of hundreds to thousands of AU from the central mass. This is particularly true for methanol (CH<sub>3</sub>OH), for which linear distributions of masers are found with disklike kinematics. In three-dimensional hydrodynamics simulations we have made to study the effects of gravitational instabilities in the outer parts of disks around young low-mass stars, the nonlinear development of the instabilities leads to a complex of intersecting spiral shocks, clumps, and arclets within the disk and to significant time-dependent, nonaxisymmetric distortions of the disk surface. A rescaling of our disk simulations to the case of a massive protostar shows that conditions in the disturbed outer disk seem conducive to the appearance of masers if it is viewed edge-on.

*Subject headings:* hydrodynamics — instabilities — masers — radio lines: ISM — stars: formation

### 1. INTRODUCTION

Masers from H<sub>2</sub>O, OH, CH<sub>3</sub>OH (methanol), and other species are commonly associated with massive protostars (Wilner & Lay 2000). In many cases, it is clear from the kinematics or location that the masers are produced in outflows and jets. However, Norris et al. (1998; see also Minier, Booth, & Conway 2000) found that some protostellar methanol masers exhibit linear alignments of multiple spots spanning hundreds to thousands of AU and have kinematics consistent with edge-on Keplerian disks around young massive stars. The circumstellar disk interpretation does not work straightforwardly for all methanol masers found near sites of high-mass star formation (Minier, Conway, & Booth 2001), but cases with linear alignments and clear-cut velocity gradients remain plausible. Masers in massive protostars due to other species may also arise in disks. For example, Shepherd & Kurtz (1999) reported H<sub>2</sub>O masers in G192.16–3.82 (IRAS 05553+1631) that appear to be located in a disk at large distances (~500 AU) from the central star (see also Lekht & Sorochenko 2001). Although less common, there are even reports of masers occurring in disks around young low-mass stars (e.g., Torrelles et al. 1998).

Numerical studies of gravitational instabilities in young stellar disks (Tomley, Cassen, & Steiman-Cameron 1991; Laughlin & Bodenheimer 1994; Pickett et al. 1998, 2000a, 2000b; Nelson et al. 1998; Boss 2000, 2001) have demonstrated that an unstable, self-gravitating disk evolving under nearly isothermal conditions fragments into a complicated time-dependent structure of dense spiral arms and arclets. When these simulations are done in three dimensions and include differential heating of the vertical disk structure by shock dissipation (Pickett et al. 2000a, 2000b), there are concomitant spiral distortions of the disk surface. Similar behavior is also evident in the 2 + 1 dimensional calculations of Nelson, Benz, & Ruzmaikina (2000). While Neufeld & Maloney (1995) have suggested that

water masers observed in the central gas disks of active galactic nuclei (AGNs; e.g., Miyoshi et al. 1995) are in molecular regions bathed in X-rays, Maoz & McKee (1998) have argued that they arise in thin postshock regions of spiral structure analogous to those found in our simulations. When we scale our relatively small and low-mass disks up to dimensions appropriate for disks in massive protostars, we find densities similar to those thought to be associated with masers. We suggest in this Letter that spiral structure due to gravitational instabilities may provide the physical basis for understanding why masers could occur in some edge-on disks of massive protostars.

### 2. NUMERICAL SIMULATION

As reviewed briefly in Boss (1998) and Durisen (2001), numerical and analytic studies over several decades have shown that gravitational instabilities set in for sufficiently small values of the Toomre parameter  $Q = c_s \kappa / \pi G \Sigma$ , where  $c_s$  is the gas sound speed,  $\kappa$  is the epicyclic frequency ( $\approx$  the disk angular rotation speed  $\Omega$ ), and  $\Sigma$  is the disk surface density. Nonaxisymmetric instabilities manifest themselves through growth of multiarmed spiral waves and occur when  $Q < \sim 1.5$ –2. When  $Q < 1$ , axisymmetric instabilities break the disk into rings. So, disk instabilities due to self-gravity occur when the disk is sufficiently cool (low  $c_s$ ) or massive (high  $\Sigma$ ). Although the equation of state (EOS) of the disk has little effect on the dynamic ( $\sim$ rotation period) growth of the instabilities, recent simulations have shown that their nonlinear outcome is critically controlled by the thermal physics of the disk (Pickett et al. 1998, 2000a; Nelson et al. 2000; Boss 2001). For conditions dominated by dissipative heating, peak amplitudes of the spiral waves are low, and the waves damp with time. For a sustained but moderate energy loss due to radiative cooling, peak amplitudes are larger, the spiral patterns are sustained, and mass transport inward occurs as a result of gravitational torques. For disks with strong radiative cooling, which evolve in a more nearly isothermal way, the disk can “fragment” into dense arms, arclets, and clumps.

#### 2.1. Initial Disk

The initial conditions for our three-dimensional hydrodynamics simulation are generated in several steps. First, an

<sup>1</sup> Department of Astronomy, Swain West 319, 727 East 3rd Street, Indiana University, Bloomington, IN 47405-7105; durisen@astro.indiana.edu, acmejia@astro.indiana.edu.

<sup>2</sup> Max-Planck-Institute for Extraterrestrial Physics, Giessenbachstrasse, 85748 Garching, Germany.

<sup>3</sup> Department of Chemistry and Physics, Purdue University Calumet, 2200 169th Street, Hammond, IN 46323; pickett@calumet.purdue.edu.

<sup>4</sup> Department of Physics and Astronomy, University of Leeds, Leeds LS2 9JT, England; twh@ast.leeds.ac.uk.

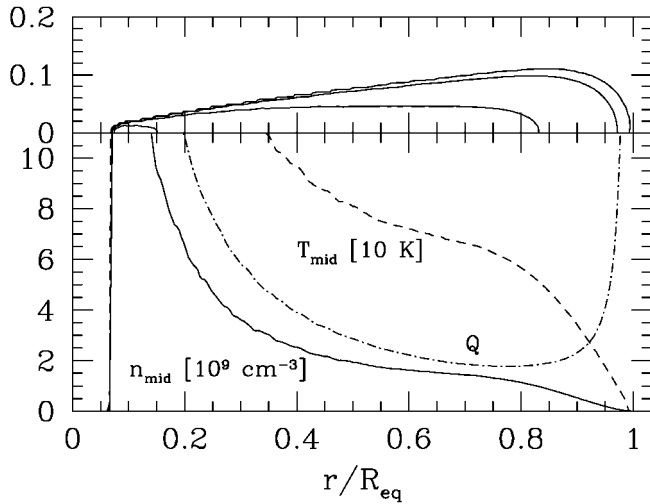


FIG. 1.—Properties of the initial disk. The top panel shows meridional contours of number density  $n$  for  $10^{10}$ ,  $10^9$ ,  $10^8$ , and  $10^7$  particles  $\text{cm}^{-3}$  from the inside out. The zero-density surface is almost identical to the outermost ( $10^7 \text{ cm}^{-3}$ ) contour shown. The bottom panel shows the radial distribution of  $Q$ , the midplane temperature  $T_{\text{mid}}$  in units of 10 K, and the midplane number density  $n_{\text{mid}}$  in units of  $10^9 \text{ cm}^{-3}$ . We use a mean molecular weight of 2.36 proton masses appropriate for a solar mix of neutral gas where the hydrogen is molecular.

axisymmetric (two-dimensional) star/disk equilibrium model with an  $n = 3/2$  polytropic EOS is created using a self-consistent field (SCF) code (Hachisu 1986; Pickett, Durisen, & Link 1997). The equilibrium structure of the thick disk and the star are fully resolved. For the calculation in this Letter, we choose a ratio of star to disk mass  $M_*/M_d = 7.08$ , a ratio of disk to stellar radius  $R_d/R_* = 20$ , and a disk surface density distribution  $\Sigma(r) \sim r^{-0.5}$ . For disks comparable in size to those observed around young low-mass stars ( $R_d \sim$  tens to hundreds of AU), it is currently impractical to include the star ( $R_* \sim$  a few  $R_\odot$ ) in a three-dimensional simulation. To remove the star, we load the SCF star/disk model into a two-dimensional hydrodynamics code and slowly cool the star/disk boundary until the disk detaches from the star. We then fix the pointlike potential due to the star and use the disk with a central hole as the initial condition of the three-dimensional simulation. Because the disk is polytropic, we can scale it to any size or mass, as long as dimensionless parameters remain fixed. Until now, we have focused on disks of solar system scales (typically tens of AU) around low-mass stars. Here we take one simulation from such a study (B. Pickett et al. 2002, in preparation) and scale it to proportions appropriate for a massive protostar,  $M_* = 20 M_\odot$ ,  $M_d = 2.8 M_\odot$ , and  $R_d = 1000$  AU. Figure 1 illustrates the meridional cross section and the radial run of various physical parameters.

## 2.2. Three-dimensional Hydrodynamics

Our second-order three-dimensional code (Pickett et al. 1998) solves the hydrodynamics equations in conservative form on a cylindrical grid of uniform spacing with  $r$ ,  $\phi$ , and  $z$  resolution of  $512 \times 128 \times 32$  with reflection symmetry about  $z = 0$ . The initial equilibrium model extends to radial zone number 242 (1000 AU), and the extra radial cells accommodate expansion of the disk due to the instabilities. The inner disk boundary is located at radial zone number 16 (50.3 AU). Outflow boundary conditions are used at the upper edge, at the outer radial boundary, and on an inner cylindrical hole (at radial zone 13); but little mass actually leaves the grid. None of the

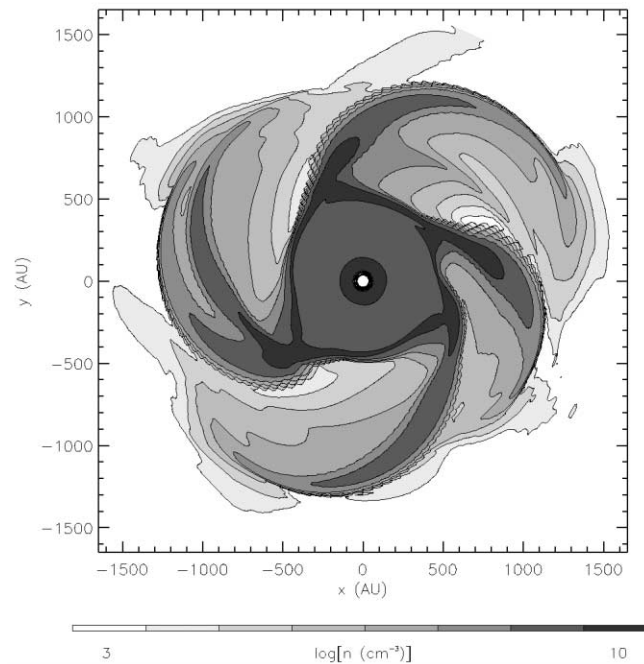


FIG. 2.—Midplane density structure of the disk after 5.1 ORPs (25,500 yr). Number density  $n_{\text{mid}}$  is represented here in a logarithmic gray scale.

restrictions on disk velocities or inner disk structure described in Boss (1998) and Pickett et al. (2000b) are imposed. The energy equation used to evolve the internal energy density  $\epsilon$  includes heating due to artificial viscosity and a volumetric cooling rate  $\Lambda$ . The gas is treated as a  $\gamma = 5/3$  ideal gas, where the pressure  $P = (\gamma - 1)\epsilon$ . For each  $r$  and  $\phi$ , we assume  $\Lambda(z) \sim \rho^\gamma$ . In the absence of shock heating, this preserves an isentropic vertical structure. The coefficient of  $\Lambda$  is set each time step so that, from  $r = 492$  AU to the outer edge of the disk, the cooling time  $t_{\text{cool}} \equiv \epsilon/\Lambda$  is 2 outer rotation periods (ORPs) of the initial disk. One ORP is 5005 yr. Inside this radial range,  $\Lambda$  tapers to zero linearly at  $r = 408$  AU. The small value of  $t_{\text{cool}}$  and its decreasing ratio to the local rotation period with increasing  $r$  mimics the short cooling times expected at large disk radii (e.g., Laughlin & Bodenheimer 1994; Boss 2001). Artificial viscosity is turned on only for  $r > 408$  AU. Disk orbital velocities range from 6.7 to 4.3  $\text{km s}^{-1}$  between 400 and 1000 AU.

## 2.3. Simulation Results

The initial disk is marginally stable (minimum  $Q \approx 1.8$ ). Low-amplitude random noise in density is superimposed on the outer half of the disk to seed nonaxisymmetric instability (see Pickett et al. 1998). In about 1 ORP, cooling makes the outer disk dynamically unstable ( $Q < 1.5$ ). Multiarmed modes reach nonlinear amplitude in the outer disk by 3.5 ORPs and develop into strong spiral arms about 1 ORP later. Figures 2 and 3 illustrate the disk structure at 5.1 ORPs. The surface distortions and dense arclike features vary on a dynamic time-scale ( $\sim$ ORP) and have associated radial motions of up to  $\pm 0.15 \text{ km s}^{-1}$ . The main result is that the outer disk develops complex spiral structure that persists for many thousands of years. As shown in Figure 1, the initial midplane number density  $n_{\text{mid}}$  in the outer disk is typically  $\sim 10^9 \text{ cm}^{-3}$ . By 5.1 ORPs, as shown in Figure 2,  $n_{\text{mid}}$  in the strong spiral structure ranges from less than  $10^5$  to more than  $10^9 \text{ cm}^{-3}$  at radial distances between 400 to 1000 AU. The spiral surface distortions high

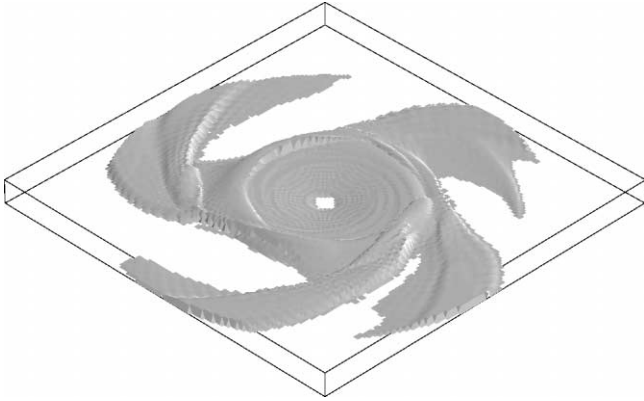


FIG. 3.—Isodensity contour of the disk after 5.1 ORPs. The upper half of the  $10^7 \text{ cm}^{-3}$  three-dimensional contour is shown from a viewing perspective of about  $45^\circ$  to the disk midplane. The reference box has dimensions of  $2116 \times 2116 \times 132 \text{ AU}$ . This is somewhat smaller than the view in Fig. 2, so some outer extensions of the spiral arms are truncated. Note the tall ridges of material in the arms.

above the midplane have number densities of the order of  $10^7 \text{ cm}^{-3}$  or more at the same radii, as shown in Figure 3. This nonaxisymmetric surface means that some lines of sight nearly parallel to the midplane can have long path lengths along dense material exposed to radiation from the star and inner disk.

### 3. DISCUSSION

#### 3.1. Maser Conditions and Chemistry

Our rescaling indicates that densities in the disk of a high-mass protostar are in the appropriate range for masering to occur at distances from the central star at which masers are seen. For instance, Gray (2001) adopted a value of  $2.5 \times 10^7 \text{ cm}^{-3}$  for the  $\text{H}_2$  number density in his work on OH masers in W3(OH). In that source, large  $\text{CH}_3\text{OH}$  maser spots are co-spatial with their OH counterparts (Menten et al. 1992). In their work on AGNs, Neufeld & Maloney (1995) found an  $\text{H}_2$  number density of the order of  $10^7 \text{ cm}^{-3}$  for AGN water masers, while Maoz & McKee (1998) derived a value of the order of  $10^9 \text{ cm}^{-3}$ . Number densities between  $10^7$  and  $10^9 \text{ cm}^{-3}$  are found in the outer parts of our disk.

In some respects, our picture is similar to that of Maoz & McKee (1998). However, in our case, the spiral shocks are far too slow to create thermal conditions favorable for masing, as they do in the Maoz & McKee scenario. Instead, we attribute the heating to the fact that, in the spiral structure, material is lifted above the disk proper, allowing it to be exposed to near-infrared radiation emitted by dust much closer to the star. At visual extinctions on the order of 100 mag and less, conditions are likely to resemble those of hot cores. In the standard picture of a hot core, the recent onset of heating releases ices from the grain mantles into the gas phase (e.g., Millar 1993; Viti & Williams 1999). The presence of large amounts of gaseous  $\text{CH}_3\text{OH}$  in many hot cores is attributed to this release, because formation by low-temperature gas-phase chemistry is inefficient. Furthermore, methanol is not produced in abundance by gas-phase chemistry in gas heated substantially by shocks (Hartquist et al. 1995), and methanol injection into the gas phase from grain mantles due to sputtering or grain-grain collisions in shocks would require the shock speed to be at least about  $10 \text{ km s}^{-1}$  (e.g., Caselli, Hartquist, & Havnes 1997). Thus, in our scenario, both the chemical and the thermal conditions favorable to the formation of  $\text{CH}_3\text{OH}$  masers are pro-

duced at the same time by the onset of near-infrared irradiation of disk material due to the spiral corrugation of the disk surface.

Speeds in the outer disk are only a few  $\text{km s}^{-1}$ . As a consequence, velocity coherence is probably not a limitation at large  $r$  for the sorts of masers we are discussing. The masers would probably tend to be seen when the disk is nearly edge-on simply because this would provide the highest surface densities and the longest path lengths for amplification.

#### 3.2. Limitations

Disks in massive protostars are poorly understood compared to their low-mass counterparts. Aside from the maser evidence itself, disks in these systems are judged to be large based on finding elongated radio continuum or hot core emission oriented perpendicular to bipolar outflows or jets (e.g., Cesaroni et al. 1999). The physical environment is probably quite complex. These disks may be associated with hot cores, or, if the central star is well developed, with an ultracompact H II region. There may also be accretion shocks near the disk surface. Little is known about density structure. Over very large scales, Cesaroni et al. suggest a steeper  $\Sigma(r)$  than we use, but the numbers are not well determined. What is clear from their observations of the disk in IRAS 20126+4104, however, is that it is very large (thousands of AU in  $\text{NH}_3$  and many hundreds of AU in  $\text{CH}_3\text{CN}$ ), contains at least several solar masses of material, is roughly Keplerian, and surrounds a massive star ( $M_* > \sim 20 M_\odot$ ).

Theoretical modeling of disk formation for massive protostars has been limited. It is generally believed that massive stars form supercritically (e.g., Shu, Adams, & Lizano 1987). Thus, their infall may become super-Alfvénic; if so, transport of angular momentum outward by hydromagnetic waves will be suppressed, leading to much greater spatial extents of these disks than for low-mass stars. Disk sizes of thousands of AU are certainly expected. For instance, the angular momentum per gram at the edge of our 1000 AU disk in Figure 1 is  $6.4 \times 10^{20} \text{ cm}^2 \text{ s}^{-1}$ , compared to  $\sim 2 \times 10^{21} \text{ cm}^2 \text{ s}^{-1}$  at the edge of a molecular cloud clump with a radius of 0.5 pc that rotates at the Galactic rotation speed. Yorke & Bodenheimer (1999) computed a detailed axisymmetric model for the collapse of a rotating  $10 M_\odot$  core. Their resulting disk is also quite large ( $\sim$ thousands of AU), is gravitationally unstable, and has a large mass ( $\sim$ several  $M_\odot$ ). Because their disk forms by collapse of an  $r^{-2}$  uniformly rotating sphere, it exhibits a much steeper  $\Sigma(r)$  in its outer region.

The structure of our disk cannot be used for detailed maser modeling because the simulation is idealized in several respects. However, our calculation does demonstrate that gravitational instabilities will lead to strong nonaxisymmetric surface distortions and that the resulting physical conditions are conducive to methanol and water maser production. The midplane cooling time due to radiation by dust from a disk with the conditions in Figure 1 is probably shorter than assumed in our simulation (Pickett et al. 2002, in preparation), and so the midplane disk would probably evolve more nearly isothermally than treated here (see Boss 2001). This would make the resulting nonaxisymmetric structure more severe. It is possible that gas giants, brown dwarfs, or even low-mass stars could be spawned from the disk under these conditions.

### 4. CONCLUSIONS

By scaling a modern three-dimensional simulation of a young stellar disk to the scale of disks expected around massive protostars, we find that vigorous gravitational instabilities are likely to occur in the outer regions of these disks (hundreds to

thousands of AU) and that these instabilities can create conditions conducive to maser emission by species such as methanol and water. In fact, as observed, masers associated with such disks are more likely to be seen when the complex spiral structure in the disk is viewed edge-on. Future simulations that include more physics could, in principle, predict the disk inclinations required to observe masers, the timescales on which spot intensity and number should vary, and the proper motions

that spots should exhibit as alignments and illumination in the disk change with time.

This work was supported by NASA Origins Program grant NAGW5-4342, by the Alexander von Humboldt Foundation, and by NASA Planetary Geology and Geophysics Program grant NAG5-10262.

## REFERENCES

- Boss, A. P. 1998, *ApJ*, 503, 923  
 ———. 2000, *ApJ*, 545, L61  
 ———. 2001, *ApJ*, 563, 367  
 Caselli, P., Hartquist, T. W., & Havnes, O. 1997, *A&A*, 322, 296  
 Cesaroni, R., Felli, M., Jenness, T., Neri, R., Olmi, L., Robberto, M., Testi, L., & Walmsley, C. M. 1999, *A&A*, 345, 949  
 Durisen, R. H. 2001, in *IAU Symp. 200, The Formation of Binary Stars*, ed. H. Zinnecker & R. Mathieu (San Francisco: ASP), 381  
 Gray, M. D. 2001, *MNRAS*, 324, 57  
 Hachisu, I. 1986, *ApJS*, 61, 479  
 Hartquist, T. W., Menten, K. M., Lepp, S., & Dalgarno, A. 1995, *MNRAS*, 272, 184  
 Laughlin, G., & Bodenheimer, P. 1994, *ApJ*, 436, 335  
 Lekht, E. E., & Sorochenko, R. L. 2001, *Astron. Rep.*, 45, 113  
 Maoz, E., & McKee, C. F. 1998, *ApJ*, 494, 218  
 Menten, K. M., Reid, M. J., Pratap, P., Moran, J. M., & Wilson, T. L. 1992, *ApJ*, 401, L39  
 Millar, T. J. 1993, in *Dust and Chemistry in Astronomy*, ed. T. J. Millar & D. A. Williams (Bristol: Inst. Physics Publishing), 143  
 Minier, V., Booth, R. S., & Conway, J. E. 2000, *A&A*, 362, 1093  
 Minier, V., Conway, J. E., & Booth, R. S. 2001, *A&A*, 369, 278  
 Miyoshi, H., Moran, J., Herrnstein, J., Greenhill, L., Nakia, N., Diamond, P., & Inoue, H. 1995, *Nature*, 373, 127  
 Nelson, A., Benz, W., Adams, F. C., & Arnett, D. 1998, *ApJ*, 502, 342  
 Nelson, A., Benz, W., & Ruzmaikina, T. V. 2000, *ApJ*, 529, 357  
 Neufeld, D. A., & Maloney, P. R. 1995, *ApJ*, 447, L17  
 Norris, R. P., et al. 1998, *ApJ*, 508, 275  
 Pickett, B. K., Cassen, P., Durisen, R. H., & Link, R. 1998, *ApJ*, 504, 468  
 ———. 2000a, *ApJ*, 529, 1034  
 Pickett, B. K., Durisen, R. H., Cassen, P., & Mejia, A. C. 2000b, *ApJ*, 540, L95  
 Pickett, B. K., Durisen, R. H., & Link, R. 1997, *Icarus*, 126, 243  
 Shepherd, D. S., & Kurtz, S. 1999, *ApJ*, 523, 690  
 Shu, F. H., Adams, F. C., & Lizano, S. 1987, *ARA&A*, 25, 23  
 Tomley, L., Cassen, P., & Steiman-Cameron, T. Y. 1991, *ApJ*, 382, 530  
 Torrelles, J. M., Gómez, J., Rodríguez, L. F., Curiel, S., Anglada, G., & Ho, P. T. P. 1998, *ApJ*, 505, 756  
 Viti, S., & Williams, D. A. 1999, *MNRAS*, 305, 755  
 Wilner, D. J., & Lay, O. P. 2000, in *Protostars and Planets IV*, ed. V. Manning, A. P. Boss, & S. S. Russell (Tucson: Univ. Arizona Press), 509  
 Yorke, H. W., & Bodenheimer, P. 1999, *ApJ*, 525, 330